Supporting Information

Highly sensitive and selective method for detecting ultratrace levels of aqueous uranyl ions by strongly photoluminescent-responsive amine-modified cadmium sulphide quantum dots

R.K. Dutta* and Ambika Kumar

Department of Chemistry, Indian Institute of Technology Roorkee, Roorkee 247667, India

* Corresponding Author: Email: duttafcy@iitr.ernet.in (R.K. Dutta)

Fax: +91-1332-286202, Tel. +91-1332-285280

All the chemicals and solvents that were used for synthesizing batches of CdS-MAA (CdS capped with only mercaptoacetic acid) and CdS-MAA-TU (CdS capped with mercaptoacetic acid and thiourea in tandem) quantum dots (QDs) are provided. The detailed method for synthesizing both the batches of CdS quantum dots and the characterization techniques employed in this study are discussed. The optimization of uranyl ion detection by the CdS quantum dots is discussed along with the analysis of spiked uranyl ion in real sample (municipal water and river water). The detailed calculation for determining the QDs with precision is explicitly demonstrated. The calculations for LoD and LoQ for QDs, interplanar distance from SAED image and XRD pattern of CdS-MAA-TU are discussed. In addition, the figures which are cited as supporting information in the manuscript are given here, e.g., the greenish-blue and bluish photoluminescence emission of the QDs when illuminated under UV light at λ =365 nm; plots showing PL intensities measured at different absorbances that were required for quantum yield calculation; XRD patterns, SAED images and FT-IR spectra of CdS-MAA and CdS-MAA-TU QDs. The plots corresponding to optimization of CdS-MAA-TU QDs for uranyl ion detection was (i.e., equilibrium time between probe and uranyl

ions) and pH of probe and analyte are given here. The zeta potentials of the probe and the probe treated with uranyl ions are given here to comment on the possible mechanism of photoluminescence quenching. A schematic representation is given to illustrate a possible interaction of uranyl ion with CdS-MAA-TU to establish the photoluminescence quenching of the probe.

EXPERIMENTAL SECTION

S 2.1 Materials. Cadmium chloride (98%, w/v), sodium sulphide (58–62%, w/v), mercaptoacetic acid (80% v/v), nitric acid (70%), sodium hydroxide (98%, w/v), and ethanol were procured from Himedia Pvt. Ltd India, while thiourea (99%) was purchased from Fluka chemika. Uranyl nitrate hexahydrate salt, arsenic acid and the sodium salts of fluoride, acetate, nitrate, chloride, carbonate, bicarbonate and sulphate were purchased from Merck, India Commercial ICP-MS standard solution of metal ions, e.g., Na^+, K^+, Mg^{2+}, Ca^{2+}, Fe^{2+}, Mn^{2+}, Pb^{2+}, Cu^{2+}, Zn^{2+}, Cd^{2+}, Co^{2+}, Cr^{3+} and Hg^{2+} were procured from Merck, India. All chemicals used in this study were not subjected to any further purification.

Synthesis of two batches of CdS quantum dots: (a) capped with mercaptoacetic acid (MAA) and (b) capped with MAA and thiourea (TU).

(a) The batch of CdS quantum dots (QDs) capped with mercaptoacetic acid (CdS-MAA) was synthesized as given in the following steps: A 0.01 M cadmium chloride solution was prepared by dissolving 50 mg of $CdCl_2.H_2O$ in 25 mL of de-ionized water (Millipore, 18 MΩ), the solution was adjusted to pH 2 by controlled addition of 200 μL of mercaptoacetic acid. The clear cadmium chloride solution turned turbid white. After 30 min of magnetic stirring, 0.1 N NaOH was added drop-wise until a clear colorless solution was obtained at pH 6. Then 25 mL of 5 mM sodium sulphide solution was added drop-wise under stirring condition. The mixture was kept

under vigorous magnetic stirring for 1 h to obtain the CdS QDs capped with MAA (i.e., CdS-MAA).

(b) For synthesizing CdS-MAA-TU QDs, the initial procedure up to the step of adding mercatoacetic acid (MAA) was same as discussed for synthesizing CdS-MAA. After 30 min of magnetic stirring, 25 mL of 5 mM thiourea (TU) was added drop-wise to the turbid solution containing the precursor cadmium chloride and MAA and was subjected for 30 min of further vigorous stirring. Then 25 mL of 0.005 M sodium sulphide was added to the above and was kept under stirring for 1 h to synthesize CdS QDs capped with MAA and TU. Both the batches of CdS nanoparticles were precipitated by adding 100 mL ethanol and separated by centrifuging at 20000 rpm for 15 min. The precipitate was washed several times with ethanol-water solution and dried at 40 $^{\text{o}}$C in oven for overnight to obtain powdered form of CdS-MAA and CdS-MAA-TU QDs. The purified powdered CdS nanoparticles were re-dispersed in de-ionized water for all optimization and analytical subsequent studies.

Characterization techniques. The X-ray diffraction patterns of the powdered batches of CdS-MAA and CdS-MAA-TU QDs were studied by Bruker AXS D8 Advance X-ray diffractometer (XRD) in 2θ range of $20 - 80^{\text{o}}$ with a scan rate of 0.2^{o} per step using Cu K$_{\alpha}$ X-ray (1.5418 Å) generated at a voltage of 40 kV. The UV-visible absorption spectra of both the batches of powdered CdS QDs re-dispersed in de-ionized water were recorded on a Shimadzu UV-1800 spectrometer and their photoluminescence emission spectra were recorded using HORIBA FluorEssence Spectrometer, equipped with a xenon lamp as the light source. The excitation and emission slit widths (2 nm) were fixed throughout the experiments. The emission spectra were recorded at an excitation wavelength (λ_{ex}) of 370 nm. Transmission electron microscopy (TEM) and the high resolution transmission electron microscopy (HRTEM) measurements were recorded on a FEI-Technai G2 microscope operated at 200 kV equipped with a CCD camera.

The samples for HRTEM imaging were prepared by drop casting a sufficiently diluted dispersion of the respective batches of CdS QDs on a copper grid and dried overnight in a desiccator. The elemental composition of the CdS QDs was determined using the X-ray detector mounted on the TEM microscope and the X-ray spectra were analyzed by GenesisRTEM software. The dynamic light scattering (DLS) and zeta potential (ζ) measurements were performed on Malvern Instrument, Nano-ZS90 (Zetasizer Nanoseries) equipped with 4 mW He-Ne laser (632 nm) light source. The Fourier transformed infrared (FT-IR) spectra were recorded on Thermo NICOLET 6700 FTIR by preparing the samples in KBr pellets.

S 2.2 Optimization, Sensitivity and Selectivity. The batches of powdered CdS QDs were conditioned at different pH in the range $3 - 8$ by diluted HNO_3 and 0.1 N NaOH solution in de-ionized water to prepare 0.075 nM quantum dot solution. Batches of different concentrations of uranyl test solutions were prepared by serial dilution of stock solution of uranyl ions (100 mg/L) in de-ionized water. The interfering metal ion stock solutions (1000 mg/L) were also prepared by serial dilution in de-ionized water and conditioned at pH 4. Similarly, 5 mM concentration of interfering anions was prepared from their respective sodium salts in de-ionized water. All photoluminescence studies in of pristine QDs and those treated with different concentrations of uranyl ions and the interfering cations and anions were performed by taking 2 mL of QDs solution and 1 mL of analyte (i.e., desired uranyl ion concentrations) or 1 mL of interfering cations and anions, respective. The contact time between the QDs and the analyte or interfering agents was optimized from kinetic study.

Real sample analysis. Two environmental water samples were studied, e.g., groundwater (Roorkee, India) and the river water (Ganga Canal, Roorkee, India). Both the samples were collected in pre-cleaned glass vessels and were filtered to avoid any particulate suspension,

before analysis. The as collected water samples were adjusted to pH 4 by dilute HNO_3 and were spiked with known concentrations of UO_2^{2+} ions (i.e., 0.5 µg/L, 5 µg/L and 10 µg/L). Batches of 2 mL of the CdS-MAA-TU QDs as probe were treated with 1 mL of groundwater or river water spiked with the known concentrations of UO_2^{2+} ions and their photoluminescence intensities were recorded after 10 min of optimized contact time.

RESULTS AND DISCUSSION

S 3.1. Quantum yield calculation:

The quantum yield was calculated using the following equation:

$$\phi_{CdS} = \frac{\phi_{Rh}(I_{CdS})(A_{Rh})}{(A_{CdS})(I_{Rh})}\frac{(\eta_{CdS})^2}{(\eta_{Rh})^2} \tag{1}$$

where, ϕ_{Rh} is the absolute quantum yield of rhodamine 6G (= 0.95). A_{CdS} and A_{Rh} are the absorbances of respective batches of CdS QDs and rhodamine-6G (Rh-6G). I_{CdS} and I_{Rh} are the corresponding integrated PL intensities of CdS QDs and Rh-6G, measured for absorbances in the range of 0.01 to 0.1. η_{CdS} and η_{Rh} represents the refractive index of the solvent used in preparing CdS QDs and dye solutions. In this study, de-ionized water was used solvent for both dye and QDs and hence the 'η' parameter was non-significant. The linear plots of integrated PL intensities against selected absorbances are shown in Figure S2A-S2C (inset represents respective photoluminescence emission spectrum).

In the equation (1), the parameter I_{Rh}/A_{Rh} corresponds to the slope of Figure S2A, which was determined to be 2.33×10^9 and the standard error of the slope was 9.54×10^7. Similarly for the batch of CdS-MAA, the parameter $I_{CdS-MAA}/A_{CdS-MAA}$ was 3.88×10^8 obtained from the slope of Figure S2B with standard error of the slope as 1.58×10^7. In the case of CdS-MAA-TU QDs, the parameter $I_{CdS-MAA-TU}/A_{CdS-MAA-TU}$ was 4.08×10^8 obtained from the slope of Figure S2C with

standard error of the slope as 1.86 x 10^7; ϕ_{Rh} = 0.95;[42] As the quantum dots and Rh-6G dye were prepared in water so η_{Rh} = η_{CdS} = 1.

Calculation of quantum yield for CdS-MAA QDs:

Substituting all the values for CdS-MAA in equation (1) we get,

$$\phi_{CdS-MAA} = \frac{0.95(3.88 \times 10^8 \pm 1.58 \times 10^7)}{(2.33 \times 10^9 \pm 9.54 \times 10^7)} \tag{1}$$

$$= 0.1582 \pm 0.0091$$

The precision of the quantum yield of CdS-MAA presented above corresponds to absolute uncertainty ($S_{\phi(CdS-MAA)}$), which is calculated as follows:

$$S_{\phi(CdS-MAA)} = (S_\phi)_{rel(CdS-MAA)} \times \phi \tag{2}$$

Where $(S_\phi)_{rel(CdS-MAA)}$ = Relative uncertainty of quantum yield of CdS-MAA

= [Relative uncertainty of $I_{CdS-MAA}/A_{CdS-MAA}$)^2 + Relative uncertainty of I_{Rh}/A_{Rh})^2]$^{1/2}$ (3)

And ϕ = Quantum yield

$$\text{Relative uncertainty of } I_{CdS-MAA}/A_{CdS-MAA} = \frac{(standard\ error\ in\ slope)_{CdS-MAA}}{(slope)_{CdS-MAA}}$$

$$= \frac{1.58 \times 10^7}{3.88 \times 10^8}$$

$$= 0.0407$$

$$\text{Relative uncertainty of } I_{Rh}/A_{Rh} = \frac{(standard\ error\ in\ slope)_{Rh}}{(slope)_{Rh}}$$

$$= \frac{9.54 \times 10^7}{2.33 \times 10^9}$$

$$= 0.0409$$

Substituting relative uncertainty values in equation (3) we get,

$(S_\phi)_{rel(CdS-MAA)} = [(0.0407)^2 + (0.0409)^2]^{1/2} = 0.0577$

Now absolute uncertainty can be calculated by substituting $(S_\phi)_{rel(CdS-MAA)}$ in equation (2),

Absolute uncertainty of quantum yield of CdS-MAA = 0.0577 x 0.1582 = 0.0091

So quantum yield (%) of CdS-MAA = 15.82 ± 0.91

Similarly, quantum yield of CdS-MAA-TU is calculated by substituting all respective parameters in equation (1):

$$\phi_{CdS-MAA-TU} = \frac{0.95(4.08 \times 10^8 \pm 1.86 \times 10^7)}{(2.33 \times 10^9 \pm 9.54 \times 10^7)} \qquad (1)$$

$$= 0.1664 \pm 0.0102$$

The uncertainty in the quantum yield for CdS-MAA-TU QDs presented above corresponds to absolute uncertainty $(S_{\phi(CdS-MAA-TU)})$, which is calculated as follows:

$$S_{\phi(CdS-MAA-TU)} = (S_\phi)_{rel(CdS-MAA-TU)} \times \phi \qquad (4)$$

where $(S_\phi)_{rel(CdS-MAA-TU)}$ = Relative uncertainty of quantum yield of CdS-MAA-TU

= [Relative uncertainty of $I_{CdS-MAA-TU}/A_{CdS-MAA-TU}$ $)^2$ + Relative

uncertainty of $I_{Rh}/A_{Rh})^2]^{1/2}$ (5)

$$\text{Relative uncertainty of } I_{CdS-MAA-TU}/A_{CdS-MAA-TU} = \frac{(standard\ error\ in\ slope)_{CdS-MAA-TU}}{(slope)_{CdS-MAA-TU}}$$

$$= \frac{1.86 \times 10^7}{4.08 \times 10^8}$$

$$= 0.0456$$

Substituting relative uncertainty values of relative uncertainty of $I_{CdS-MAA-TU}/A_{CdS-MAA-TU}$ and I_{Rh}/A_{Rh} in equation (5) we get relative uncertainty of quantum yield of CdS-MAA-TU:

$(S_\phi)_{rel(CdS-MAA-TU)} = [(0.0456)^2 + (0.0409)^2]^{1/2} = 0.0612$

Therefore from equation (4),

 Absolute uncertainty of quantum yield of CdS-MAA-TU = 0.0612 x 0.1664 = 0.0102

So quantum yield (%) of CdS-MAA-TU = 16.64 ± 1.02

S 3.2. Determination of the inter-planar distance from SAED and XRD measurements of CdS-MAA-TU QDs

(i) SAED image analysis (from Figure S3):

Radius of the ring (R in1/ nm),	δ = 1/R (in nm)	atomic plane
3.12	0.321	(111)
4.73	0.211	(220)

(ii) XRD data analysis of CdS-MAA-TU: (Figure S1 in supporting file)

2θ values (in degree)	atomic plane	Inter-planar distance (nm)
27.8^o	(111)	δ = 1.54 Å/(2sin13.9)
		= 3.53 Å
		= 0.353 nm
46.4^o	(220)	δ = 1.54 Å/(2sin 23.2)
		= 2.16 Å
		= 0.216 nm

S 3.3 (i) Calculation of limit of detection (LoD) and limit of quantification (LoQ):

LoD = 3σ/the slope of the linear region of calibration

where σ corresponds to the standard deviation of the photoluminescence peak for only probe.

(3σ is used to have 99.7% confidence that any reading above this is not a noise).

The photoluminescence intensities of 5 batches (P_1 to P_5) of probe solution (measured at $\lambda = 505$ nm and $\lambda = 480$ nm for CdS-MAA and CdS-MAA-TU batches respectively) are:

Probe	P_1	P_2	P_3	P_4	P_5	σ
CdS-MAA	33266.836	33266.850	33266.835	33266.834	33266.852	0.008790
CdS-MAA-TU	36507.756	36507.750	36507.763	36507.769	36507.759	0.007203

σ : standard deviation from 5 measurements (as above)

$\sigma_{(CdS\text{-}MAA)} = 8.79 \times 10^{-3}$

$\sigma_{(CdS\text{-}MAA\text{-}TU)} = 7.203 \times 10^{-3}$

$\text{LoD (for CdS-MAA)} = \dfrac{3\sigma_{CdS-MAA}}{Slope_{CdS-MAA}}$ (σ is calculated using the formula given below in section ii)

$= \dfrac{3 \times 8.79 \times 10^{-3}}{0.0053}$ (From Figure 3A)

$= 4.98\ \mu g/L$

Similarly, $\text{LoD (for CdS-MAA-TU)} = \dfrac{3\sigma_{CdS-MAA-TU}}{Slope_{CdS-MAA-TU}}$

$= \dfrac{3 \times 7.20 \times 10^{-3}}{0.316}$ (From Figure 3C)

$= 0.07\ \mu g/L$

Limit of Quantification (LoQ) = 3.3 x LoD,

LoQ (for CdS-MAA) = 3.3 x 4.98 = 16.43 µg/L,

And LoQ (for CdS-MAA-TU) = 3.3 x 0.07 µg/L = 0.231 µg/L

(ii) <u>Formula used for calculating accuracy and precision of reported data:</u>

All analytical results in the manuscript are presented as mean ± standard deviation of triplicate measurements.

Mean value is calculated as:

$$mean\ value = \frac{(x_1 + x_2 + x_3)}{3}$$

Where, x_1, x_2 and x_3 are the independent measurements

The standard deviation is taken as the precision of the three independent measurement, given as:

$$Standard\ deviation\ (\sigma) = \sqrt{\left[\frac{(x_1 - \bar{x})^2 + (x_2 - \bar{x})^2 + (x_3 - \bar{x})^2}{2}\right]}$$

Figures as Supporting Information
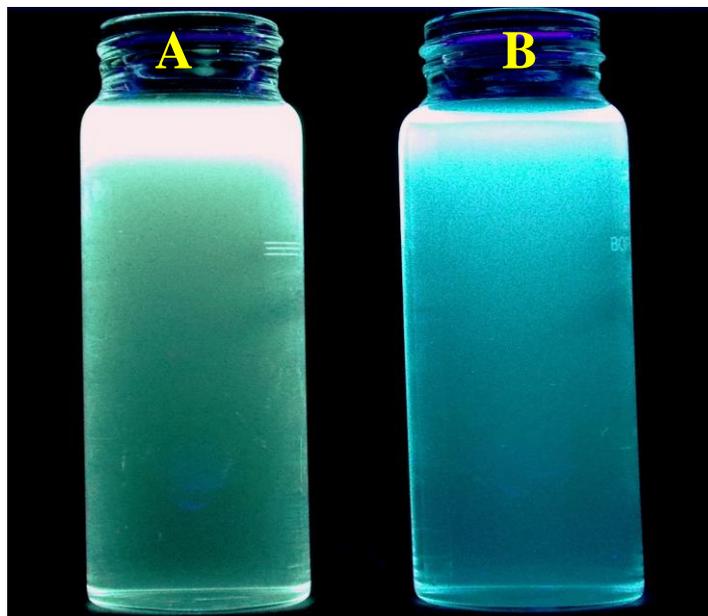
Figure S1. (A) Greenish-blue photoluminescence emission by CdS-MAA QDs and (B) bluish photoluminescence emission by CdS-MAA-TU QDs under illumination at λ=365 nm UV light
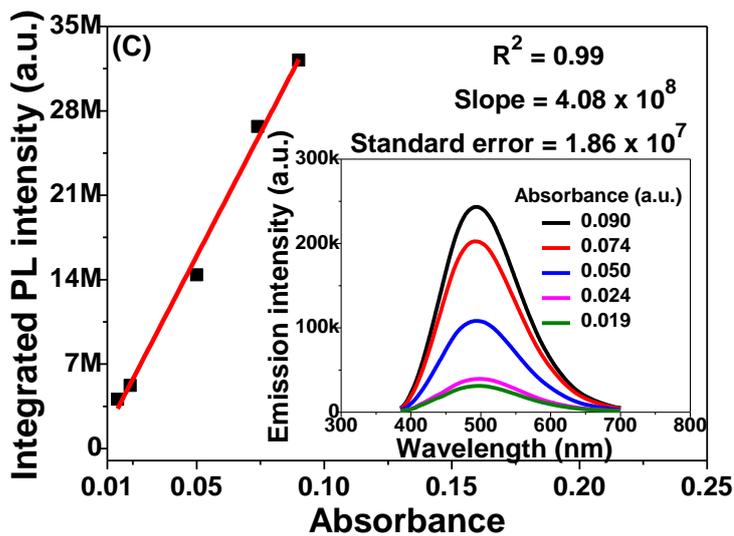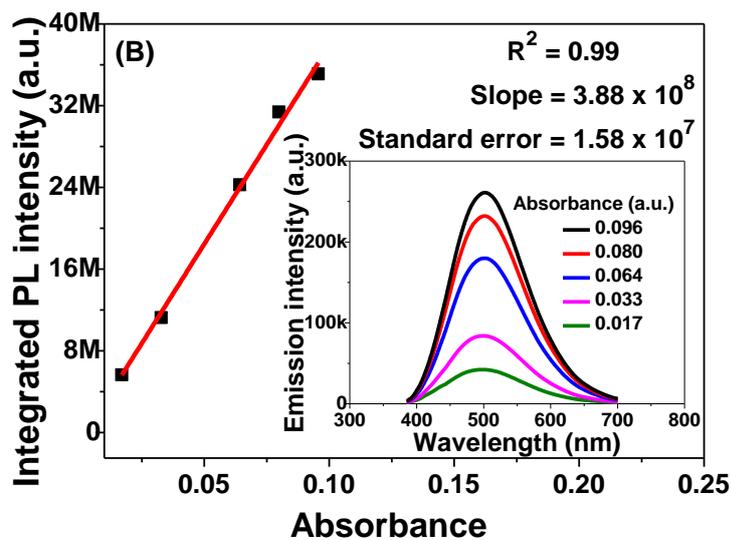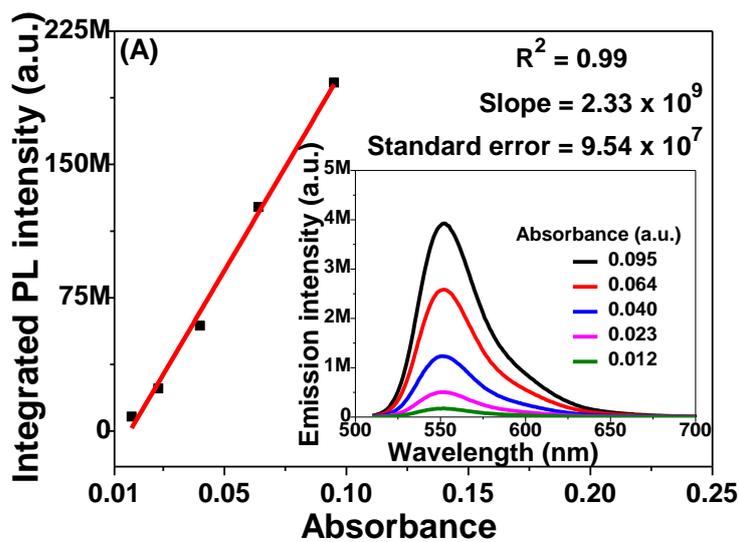
Figure S2 Plots showing linear relationship between integral photoluminescence (PL) intensity at respective absorbances for (A) Rhodamine 6G dye, (B) CdS-MAA and (C) CdS-MAA-TU. Inset in each plot showing photoluminescence spectra recorded at selected absorbances.
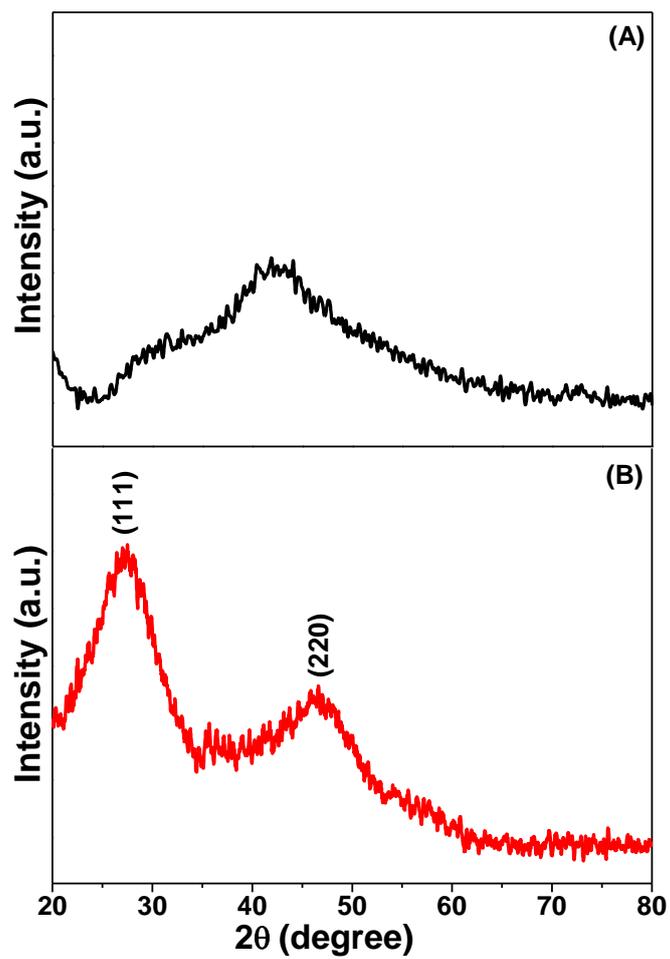
Figure S3. XRD pattern of powdered (A) CdS-MAA and (B) CdS-MAA-TU QDs
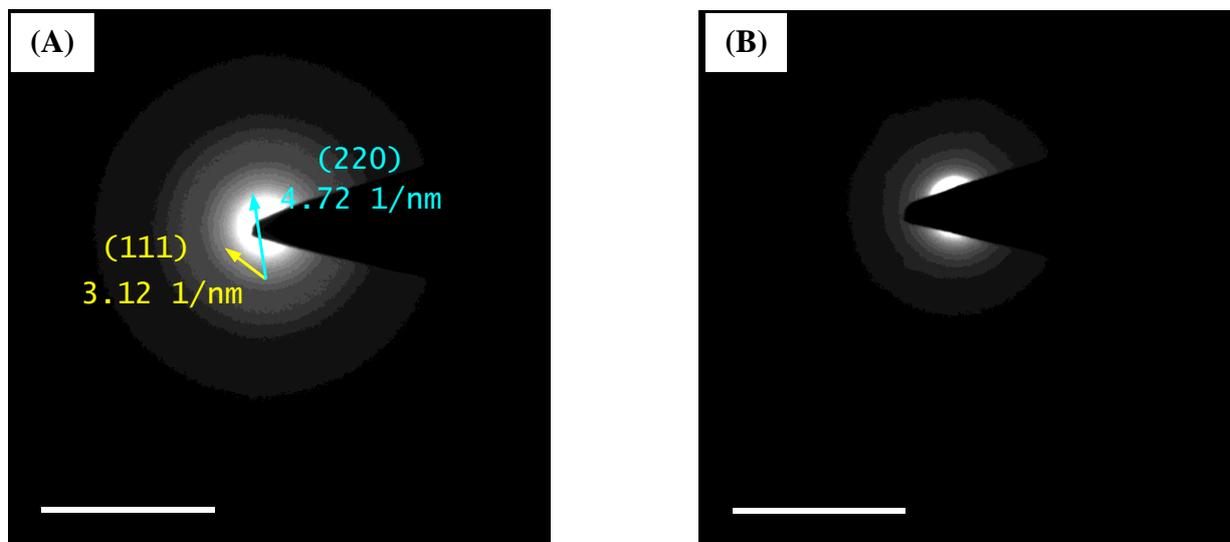
Figure S4. SAED pattern of (A) CdS-MAA-TU and (B) CdS-MAA
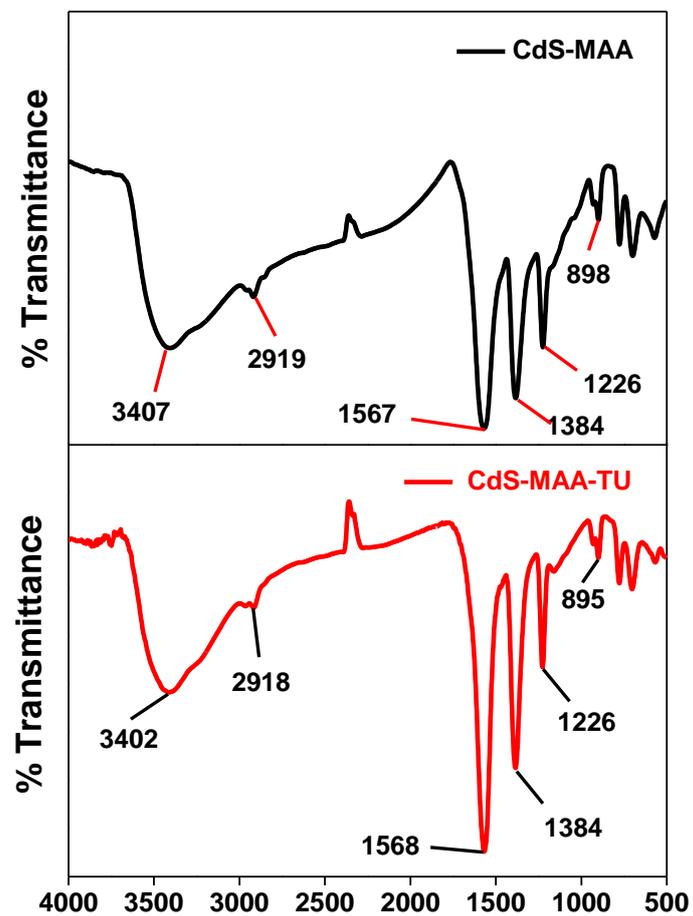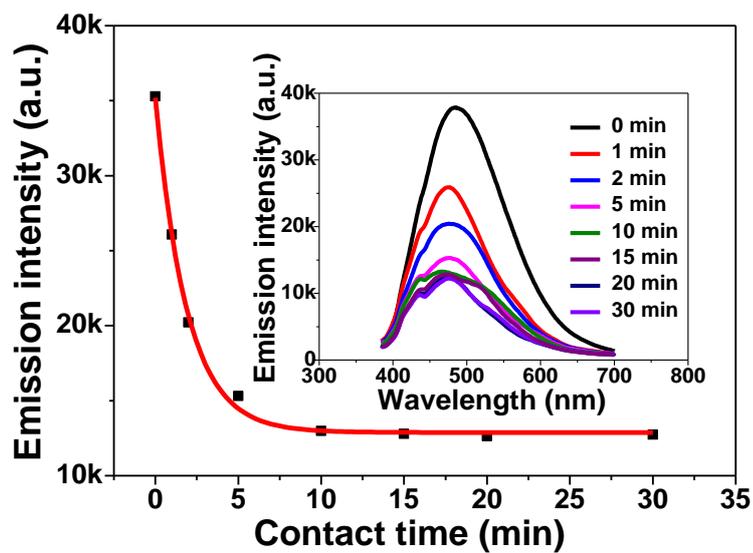
Figure S5. FT-IR spectrum of CdS-MAA (upper panel) and CdS-MAA-TU (lower panel)

Figure S6. Photoluminescence property of CdS-MAA-TU treated with 5 µg/L uranyl ions as a function of time. Inset showing photoluminescence spectra of CdS-MAA-TU treated with 5 µg/L uranyl ions at selected time.
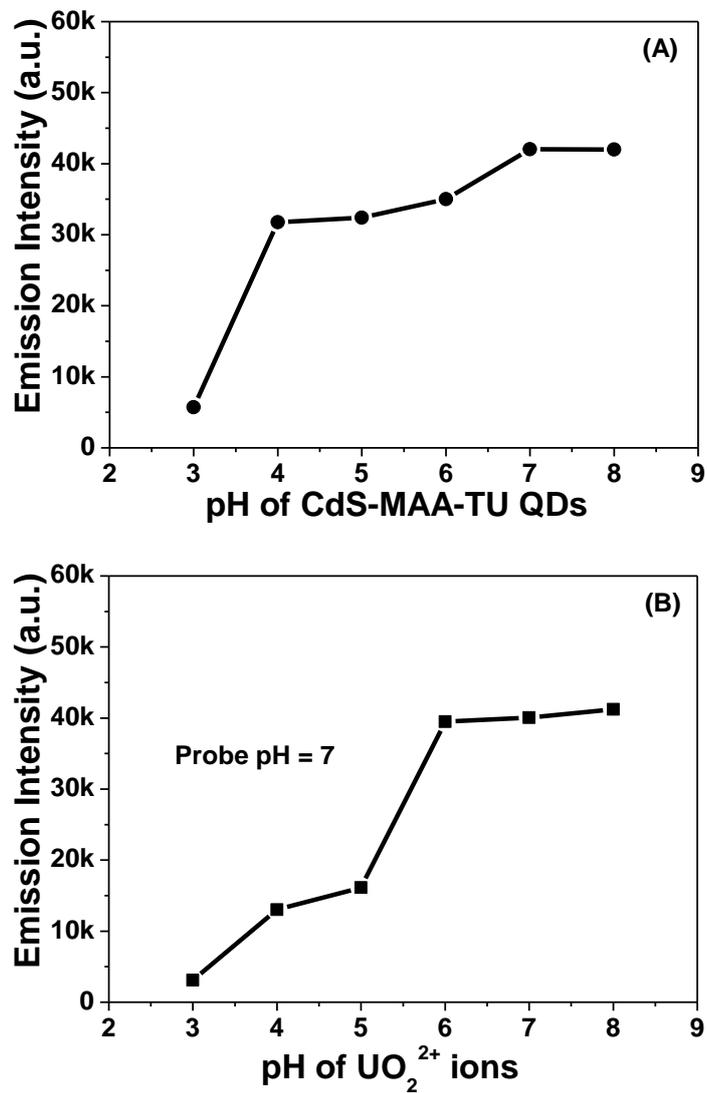
Figure S7 Photoluminescence emission intensities of (A) only CdS-MAA-TU QDs as probe at different pH (B) CdS-MAA-TU QDs as probe at pH 7 treated with 5μg/L of UO_2^{2+} ions at pH ranging between 3 and 8
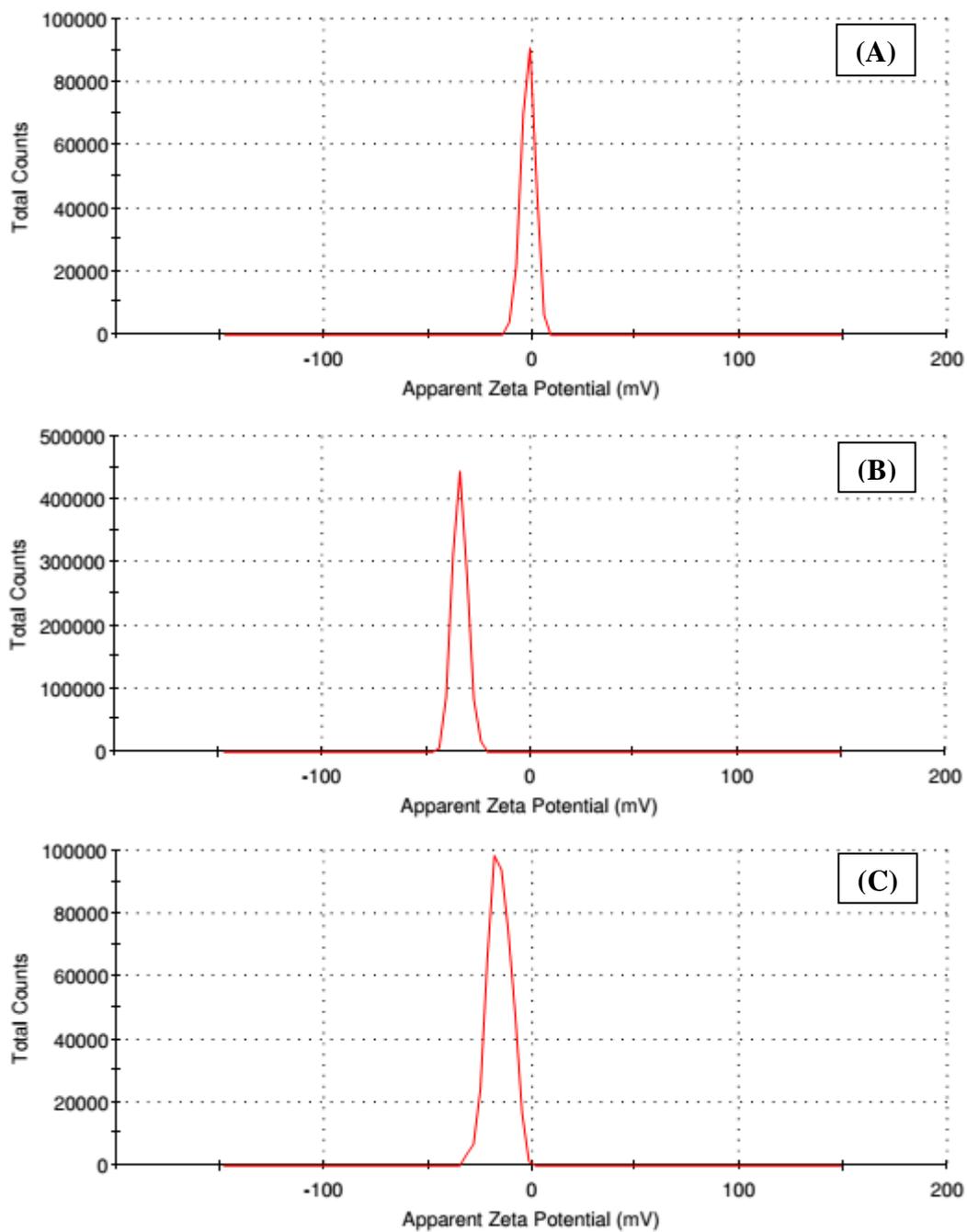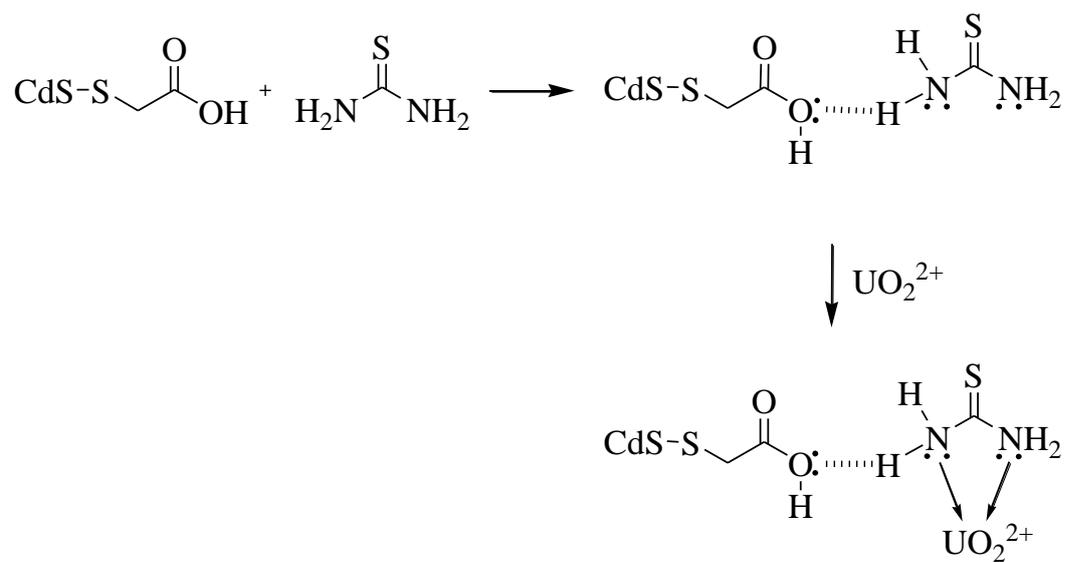
Figure S8. Zeta potential measurement of CdS-MAA-TU DQs at (A) pH 3 = -1.94 mV; (B) pH 7 = -33.8 mV (C) after equilibration with 200 μg/L of UO_2^{2+} = -15.7 mV

Scheme 1: Representing interaction of UO_2^{2+} ions with amine groups of thiourea in CdS-MAA-TU QDs